

**Sodium vacancy ordering and the co-existence of localized spins
and itinerant charges in Na_xCoO_2**

F. C. Chou^{1,2}, M. -W. Chu¹, G. J. Shu¹, F. T. Huang^{1,3,4}, Woei
Wu Pai¹, H. S. Sheu², T. Imai⁵, F. L. Ning⁵, & Patrick A. Lee⁶

¹*Center for Condensed Matter Sciences,
National Taiwan University,
Taipei 10617, Taiwan,*

²*National Synchrotron Radiation Research Center,
HsinChu 30076, Taiwan,*

³*Taiwan International Graduate Program,
Academia Sinica, Taipei 115, Taiwan,*

⁴*Department of Chemistry,
National Taiwan University,
Taipei 10617, Taiwan,*

⁵*Department of Physics and Astronomy,
McMaster University, Hamilton,
ON L8S4M1, Canada,*

⁶*Department of Physics,
Massachusetts Institute of Technology,
Cambridge, MA 02139*

Abstract

The sodium cobaltate family (Na_xCoO_2) is unique among transition metal oxides because the Co sits on a triangular lattice and its valence can be tuned over a wide range by varying the Na concentration x . Up to now detailed modeling of the rich phenomenology (which ranges from unconventional superconductivity to enhanced thermopower) has been hampered by the difficulty of controlling pure phases. We discovered that certain Na concentrations are specially stable and are associated with superlattice ordering of the Na clusters. This leads naturally to a picture of co-existence of localized spins and itinerant charge carriers. For $x = 0.84$ we found a remarkably small Fermi energy of 87 K. Our picture brings coherence to a variety of measurements ranging from optical to thermal transport. Our results also allow us to take the first step towards modeling the mysterious “Curie-Weiss” metal state at $x = 0.71$. We suggest the local moments may form a quantum spin liquid state and we propose experimental test of our hypothesis.

Sodium cobaltate (Na_xCoO_2) has received a great deal of attention from the condensed matter physics and materials science communities recently because the cobalt valence can be tuned over a great range by varying the Na concentration, leading to unusual properties all the way from unconventional superconductivity when hydrated[1] at $x \approx 0.3$ to a novel “Curie-Weiss metal”[2] for $x \approx 0.7$ to enhanced thermopower[3] for $x \approx 0.85$. Here we concentrate on $x > 0.5$ where unusual magnetism[4] has been observed and the ordering of the Na ions is thought to play an important role.[5, 6, 7, 8] Through electrochemical de-intercalation and a careful characterization of the Na concentration on high purity single crystals, we determine that there is a special island of stability at $x = 0.71 \pm 0.01$. We also studied $x = 0.84 \pm 0.01$ which is the limit of single phase stability for high temperature melt growth. Using x-ray and electron diffraction, we determine that these two phases exhibit special Na ordering patterns. We discovered a hexagonal $\sqrt{13}a \times \sqrt{13}a$ superstructure for $x = 0.84 \approx 11/13$, leading naturally to a picture of ordered di-vacancies. For $x = 0.71$, we find a hexagonal $\sqrt{12}a \times \sqrt{12}a$ superlattice which contains 12 unit cells. Due to the unique triangular cobalt lattice structure and its stacking sequence, we find a special stability for a model of alternating layers of Na tri-vacancy and quadri-vacancy, so that $x = 0.71$ is understood to be the average of $3/4$ and $2/3$ doping. These results are supported by ^{23}Na NMR. Our analysis builds on the vacancy clustering model suggested by Roger *et al.*[9] However our finding that tri- and quadri-vacancies are more stable at smaller x than di-vacancies is contrary to their proposal.

Our picture of the Na vacancy leads naturally to an electronic model where a fraction of Co^{4+} holes are bound to Na vacancies, resulting in the co-existence of $S = \frac{1}{2}$ local moments and itinerant carriers. For $x = 0.84$, we find an extremely low Fermi temperature of 87 K for the itinerant carriers which may explain the high thermopower and the emergence of ferromagnetism in the layer. For $x = 0.71$, we suggest that the Curie-Weiss metal may be indicative of a novel quantum spin liquid phase for the local moments.

Na ions are easily lost during high temperature preparation,[10] and they continue to diffuse to the surface layer even after stoichiometric sample is fully reacted and stored at room temperature.[14] Adding extra Na into the precursor has been a common practice in the powder sample preparation in order to compensate for the high temperature Na loss. Alternatively “rapid heat-up” technique is applied to reduce Na loss.[10] However neither method can control Na level to the nominal concentration perfectly within a few percent

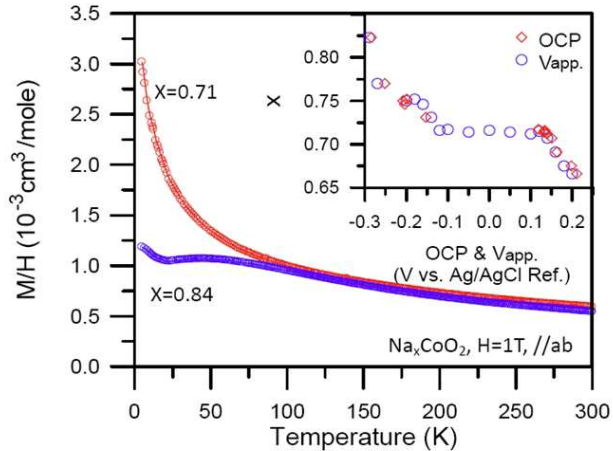


FIG. 1: **Spin susceptibilities and preparation method.** The spin susceptibility for field parallel to the ab plane for single crystal samples of $x = 0.71$ and 0.84 . Note the strong increase for $x = 0.71$ at low temperatures. The inset shows the open circuit potential (OCP) and the applied potential V_{app} in our electrochemical cell. The step at $x = 0.71$ indicates a concentration of special stability.

error while 3-4 % difference would introduce a completely different vacancy ordering patterns. Many inconsistent results reported between $x = 0.67 - 0.85$ before are due to inaccurate Na content or inconsistent ordered patterns. Thanks to the much lower surface-to-bulk ratio in single crystal form, we believe structure work based on single crystal prepared using room temperature de-intercalation method is the most reliable route to study Na (vacancy) ordering. The Na concentration of single crystal sample in this study has been checked thoroughly using Electron Microprobe Analysis (EPMA) from more than 10 points from freshly cleaved surface and c-axis parameters are calibrated against to those reported in the literature. Combining our series of single crystal samples calibrated with EPMA[14] and the reported powder sample calibrated with ICP analysis,[2] the c-axis versus Na content relationship falls into a linear relationship of $c = -0.9866x + 11.639$ in the range of $0.6 \leq x \leq 0.84$. As a byproduct of the present paper, we can recommend with confidence the use of this c-axis formula as a way of determining x . This scale is anchored at two special points, $x = 0.71$ and $x = 0.84$ where the c axes are 10.939\AA and 10.810\AA , respectively. As we shall see, based on the superlattice structure as supported by NMR, we arrive at these x values independent of EPMA analysis.

γ phase Na_xCoO_2 is prepared by chronoamperometry technique on single crystal sample in electrochemical cell constructed as $Na_xCoO_2/1N NaClO_4$ in propylene carbonate/Pt.[14] Starting from the original crystal $Na_{0.84}CoO_2$ grown with floating-zone method, constant anodic potential is applied to the sample electrode until the induced current decays to zero. The concentration x has been carefully determined by freshly cleaved surface using EPMA. The applied voltage (V_{app}) for preparation and its final equilibrated open circuit potential (OCP) versus x is summarized in Fig.1. The most prominent feature in Fig.1 is the step at $x = 0.71$ vs applied voltage, indicating that $x = 0.71$ is an exceptionally stable phase. This is very surprising because the naive expectation is for steps at rational fractions such as $\frac{3}{4}$ or $\frac{2}{3}$, but such steps are either weak or non-existent.

Another indication that $x = 0.71$ is a specially ordered structure comes from the fact that crystals of exceptional homogeneity can be grown at this concentration. The residual resistivity of $x = 0.71$ is low among the cobaltate family[2] and has been measured by M. Lee and N. P. Ong to be as low as $8\mu\Omega\text{-cm}$ at 0.3 K in our crystals. This is seven times lower than commonly reported in the literature[15] and corresponds to $k_F\ell = 220$ where ℓ is the mean free path. The special order also leads to narrow NMR lines which we will take advantage of later.

Another special concentration is $x = 0.84$, which is the as-grown material obtained using optical floating-zone technique.[13] For x greater than 0.84 we generally find mixed phases, in agreement with the observation by Lee *et al.*[3] Between $x = 0.75$ and 0.84 we find single phase with a magnetic phase transition around 20 K. At $x = 0.84$ the transition moves up to 27 K. The magnetic order is known to be A type, with ferromagnetic order in plane and antiferromagnetic between neighboring Co planes.[4] This has presented a puzzle, because the spin susceptibility for $x = 0.84$ powder average above 100 K (see Fig.1) shows a Curie-Weiss fit $\chi = \chi_0 + C/(T - \theta)$ with $\theta \approx -77$ K, characteristic of antiferromagnetic exchange. At $x = 0.71$ the magnetic order disappears. The spin susceptibility above 100 K is very similar to that of 0.84, but keeps rising at low temperatures. Data below 60 K can be fitted by a Curie-Weiss law with $C \approx 0.04 \text{ cm}^3 \text{ K/mole}$ and $\theta \approx -12$ K. This rise is much stronger than previously reported. [2] The resistivity shows a linear T behavior below 100 K and becomes T² only below ≈ 4 K.[15] The name ‘‘Curie-Weiss’’ metal has been given to this

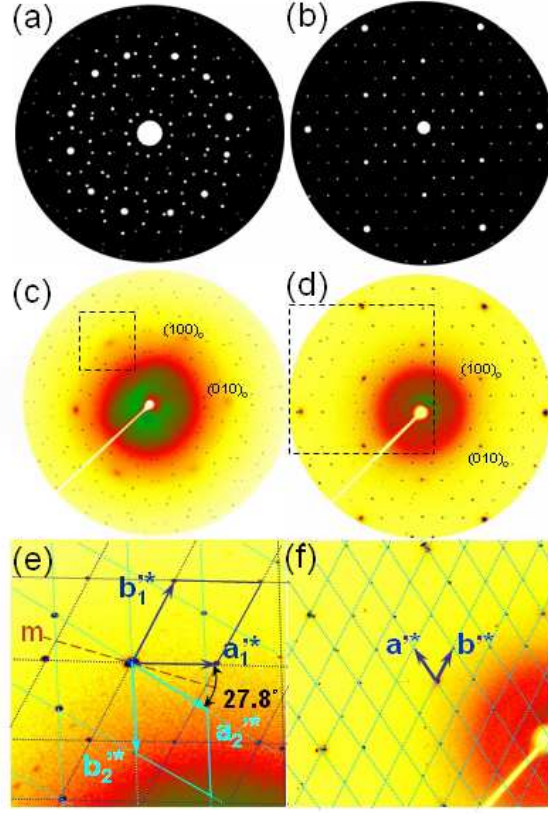


FIG. 2: Single crystal synchrotron X-ray diffraction and analysis The Laue patterns for (c) $x = 0.84$ and (d) $x = 0.71$ and the corresponding simulated diffraction patterns (a) and (b). Note the 12 member ring for $x = 0.84$ in (c) and the simple hexagonal superstructure for $x = 0.71$ in (d). (e) is a blow up of the dashed region in (c) showing that the superstructure for $x = 0.84$ can be indexed with two sets of \mathbf{a}^* in k-space ($\sqrt{13}a$ in real space) of 27.8° separation with a mirror plane. (f) is a blow up of the dashed region in (d) showing single domain indexed for $x = 0.71$, which corresponds to a hexagonal superlattice of $\sqrt{12}a$ in real space. highly unusual combination of magnetic and transport properties.[2] Due to their special properties and stability, we focus our attention on $x = 0.84$ and 0.71 .

We performed transmission Laue X-ray diffraction study on single crystal Na_xCoO_2 with $x = 0.84$ and 0.71 using synchrotron source of Taiwan NSRRC. Superlattice diffraction spots appear near the original $P6_3/mmc$ structure indices $\{100\}$, $\{110\}$ and $\{200\}$ as shown in Fig.2. For $x = 0.84$ we found a hexagonal $\sqrt{13}a \times \sqrt{13}a$ superlattice structure. The major character of this Laue pattern is the 12 spots ring that formed near $\{100\}$ peaks of the original lattice. As shown in the Fig.2(c), these spots consist of 2 sets of six-fold rings

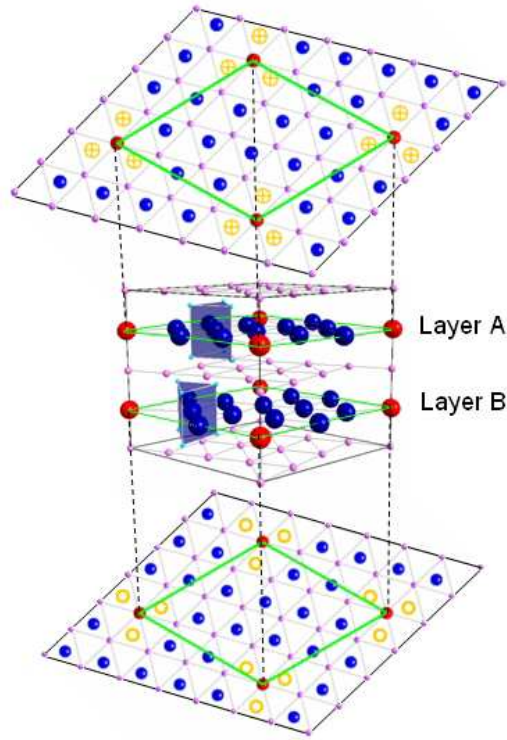


FIG. 3: **2d and 3d structure model of $Na_{0.84}CoO_2$.** The middle panel shows the unit cell of $Na_{0.84}CoO_2$, where oxygen atoms are removed for better viewing, except for the prismatic cage near Na2. The Na2 site (blue) sits at the center of an oxygen prism (shaded blue) which is shifted between the two layers of the unit cell. The Na1 site (red) sits directly above and below Co (light blue). Top and bottom panels show the 2D view of the top(A) and bottom (B) Na layers. The green lines show the $\sqrt{13}a \times \sqrt{13}a$ superlattice formed by the di-vacancy which is centered on the Na1 site surrounded by 3 empty Na2 sites (yellow).

rotated by $\sim 28^\circ$, where each set is indexed using two simple hexagonal unit cells with $a' = \sqrt{13}a$. Direct evidence of this model comes from electron diffraction with a beam size of 150 – 200 nm, which shows 6-fold rings coming from one of two domains. Details are discussed in the supplementary section. Fig.2(a) shows the simulated diffraction pattern along the c-axis for $x = 0.84$, where the agreement using two-domain simulation is high even before the intensity is corrected by the refined Na2 position and the associated structure factors. The $\sqrt{13}a \times \sqrt{13}a$ structure corresponds precisely to the ordering of di-vacancies shown in Fig.3. With one di-vacancy per 13 cobalt, we predict $x = 1 - \frac{2}{13} = 0.846$ which agrees with $x = 0.84 \pm 0.01$ measured with EPMA within error.

We note that Roger *et al.*[9] reported very similar 12 spot ring diffraction patterns for what they labeled as $x = 0.75$. However, they fitted the pattern with a 15-site monoclinic superstructure which contains one tri-vacancy. This model gives a Na content of $x = 1 - \frac{3}{15} = 0.8$, inconsistent with $x = 0.75$. We suspect that their sample grown by high temperature quench may suffer from inhomogeneity and uncertainty with respect to x determination. It will be useful to check if their pattern can also be indexed with our structure model.

Next we discuss the stacking properties of the Na vacancies. We first review the salient feature of the parent $\gamma - Na_xCoO_2$ lattice of $P6_3/mmc$ symmetry using $x = 0.84$ unit cell as shown in Fig.3. The unit cell consists of two layers of cobalt atoms located directly on top of each other and layers of Na atoms sandwiched in between. There are two Na sites in each layer, called Na1 at $(0,0,\frac{1}{4})$ and Na2 $(\frac{2}{3},\frac{1}{3},\frac{1}{4})$, the latter being the preferred site because Na1 sits directly on top of the positively charged Co and is more costly electrostatically. Na2 sits in the center of a prismatic cage formed by six oxygens in each layer, and the two Na layers (labeled A, B) are distinguished by the different position of these prismatic cages. In addition to the Na sites, there are sites sitting directly under oxygen which we refer to as O sites. Note that in layer A the Na2 and O sites occupy the center of the down and up pointing triangles, respectively, but their positions are interchanged when we go from layer A to layer B. This will have crucial consequences later. The di-vacancy is formed by creating three Na2 vacancies (shown in yellow) and then occupying a Na1 site.[9] Since the di-vacancies are centered on the Na1 site, they can stack directly on top of each other, going from layer A to B. On the other hand, out of phase stacking, for example by placing the di-vacancy at the center of the green diamond shown in Fig.3 produces ambiguity because two such sites are equivalent. This will lead to disorder. At present it is not possible to distinguish between in phase and out of phase stacking by refinement.

Next we turn to the $x = 0.71$ sample which, as mentioned earlier, is special in its stability. Density Function Theory (DFT) model calculations indicate special stability for $x = 5/7 = 0.714$ and our initial expectation was to search for hexagonal $\sqrt{7}a \times \sqrt{7}a$ superstructure of di-vacancies.[16] Instead, we discovered hexagonal superstructure at $\sqrt{12}a \times \sqrt{12}a$ which contains 12 Na2 sites per unit cell per layer. We are then led to consider tri- and quadri-vacancies in order to account for the 0.29 missing Na ions. These vacancies were described by Roger *et al.*[9] and shown in Fig.4, where we emphasize the special role of A,B stacking. The tri- and quadri-vacancies consist of Na1 trimers surrounded by six and seven Na2 vacancies

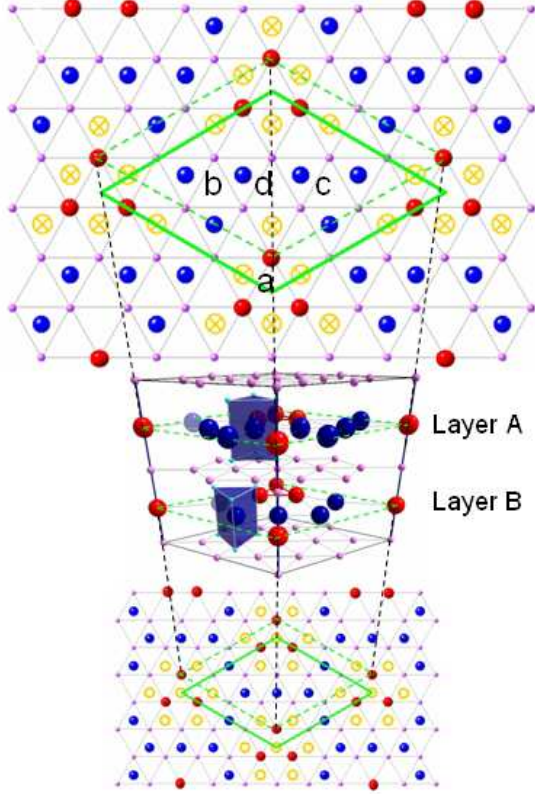


FIG. 4: **2d and 3d structure model of $Na_{0.71}CoO_2$.** The unit cell for $x = 0.71$ before considering the 3c stacking. The $\sqrt{12}a$ superlattice structure of tri-vacancy in layer A and quadri-vacancy in layer B are shown with green solid lines. Note the vacancies consist of Na1 trimers surrounded by empty Na2 sites (yellow circles).

(shown in yellow), respectively. Note that the trimer in the tri-vacancy is centered on the O site while the trimer in the quadri-vacancy is centered on the Na2 site. Recall that the role of O and Na2 sites are reversed between layers A and B. This has the remarkable consequence that tri- and quadri-vacancies can stack coherently, e.g. they can either (i) stack in phase, with tri-vacancy and quadri-vacancy sitting directly on top of each other, or (ii) stack out of phase, with tri-vacancy on site a in layer A and quadri-vacancy either directly below the d site or below the b,c sites. (these sites are defined in Fig 4.) The alternating stacking of tri- and quadri-vacancies lead to $x = 1 - \frac{1}{2} \left(\frac{3+4}{12} \right) = 0.708$. We believe the special stacking property described above is responsible for the exceptional stability of the 0.71 Na concentration.

We expect out of phase stacking to be more favorable by electrostatic consideration. In

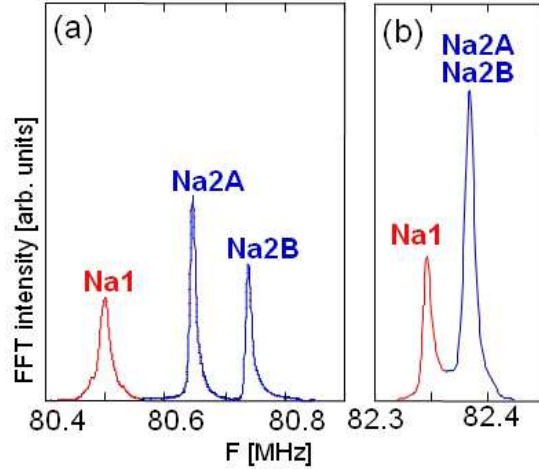


FIG. 5: ^{23}Na NMR spectra for $\text{Na}_{0.71}\text{CoO}_2$. ^{23}Na NMR spectra for $x = 0.71$ taken at 20 K. Applied field $B = 7.298$ Tesla is parallel to the c -axis. (a) the $\pm\frac{3}{2}$ to $\pm\frac{1}{2}$ satellite transitions, and (b) the $(-\frac{1}{2} \rightarrow \frac{1}{2})$ central transitions.

this case the c -axis periodicity could be multiplied due to a versatile AB stacking combinations, e.g. A_aB_b (c), $A_aB_bA_aB_c$ (2c) or $A_aB_bA_cB_aA_bB_c$ (3c). We have found evidence of 3c modulation through both single crystal electron diffraction as well as synchrotron X-ray powder diffraction techniques, which is discussed in detail in the supplementary section. The evidence of 3c modulation supports $A_aB_bA_cB_aA_bB_c$ stacking and indicates that simple electrostatic consideration dominates the stacking sequence of vacancy cluster units between layers.

We next consider stacking of tri-vacancies in the AB layers (TT) to form $x = 1 - \frac{1}{2}(\frac{3+3}{12}) = 0.75$, or stacking quadri-vacancies (QQ) to form $x = 1 - \frac{1}{2}(\frac{4+4}{12}) = 0.67$. Note that unlike the 0.71 case considered earlier, there are now three equivalent choices to stack the center of Na1 trimers in the case of TT and QQ stacking. This is true for both in-phase and out-of-phase stacking. Such triangular ambiguity introduces significant disordering for the TT and QQ vacancy clusters, which could be the major reason why $x = 0.71$ is the most stable phase among these three types of stacking. Indeed, as shown in Fig.1, the stability range for $x = 0.75$ and 0.67 are relatively narrow as indicated by the $dx/V_{app} = 0$ plateau in the electrochemical preparation.

We have also performed ^{23}Na NMR measurements of $x = 0.71$ crystal. The central transition $(\frac{1}{2} \rightarrow -\frac{1}{2})$ and the lower satellites $(\pm\frac{3}{2} \rightarrow \pm\frac{1}{2})$ are shown in Fig. 5. These lines

are considerably narrower than what were previously reported in the literature,[5, 6] and are also narrow compared with our crystals at other Na concentrations. The central line in Fig. 5(b) separates into two groups with different Knight shifts and we assign the minority as Na1 as indicated in the figure. The satellite peaks of Na2 further split into two peaks, Na2A and Na2B, due to the difference in the nuclear quadrupole interaction. We measured the weight of the Na1 : Na2A : Na2B lines to be 36.3% : 37.1% : 26.5% with an error of $\pm 3\%$. In our structure model we have three Na1 and six Na2 in layer A (tri-vacancy layer) and three Na1 and five Na2 in layer B (quadri-vacancy layer). The Na1 form trimers and have similar environments in both layers. The total fraction of Na1 is predicted to be $\frac{3+3}{3+3+6+5} = 35.3\%$, in excellent agreement with observation. We emphasize that the sharpness of the lines allows accurate weight determination which can be used to rule out other structure models. For example, if layer B were to contain two di-vacancies instead of a single quadri-vacancy per unit cell, leaving the x value unchanged, that layer would have two Na1 and six Na2 sites and the total fraction of Na1 is predicted to be $\frac{3+2}{3+2+6+6} = 29.4\%$, inconsistent with the measured value. Generally, the existence of di-vacancy and mono-vacancy will decrease the Na1 fraction beyond what is permissible, giving us great confidence in our assignment of tri- and quadri-vacancy to $x = 0.71$. We also note that the six Na2 sites have identical environments in layer A, while in layer B five Na2 are separated into two groups of 2 sites with three Na2 nearest neighbors and 3 sites with two Na2 and one Na1 nearest neighbors. Provided that the splitting of the latter group is not resolved, it is tempting to assign the Na2A and Na2B lines to the A and B layers, respectively, in which case the weight ratio of Na1 : Na2A : Na2B is predicted to be $6 : 6 : 5 = 35.3\% : 35.3\% : 29.4\%$, within error of the observation.

What are the consequences of the Na superstructure order for the electronic properties of the cobalt oxide planes? First we consider $x = 0.84$. Starting from the band insulator $NaCoO_2$, there are $2/13$ holes in an otherwise filled band. It is natural that one hole will be bound to each di-vacancy, forming a localized $S = \frac{1}{2}$ spin. The second hole remains itinerant, explaining the metallic nature of this state. This leads to a model of local moments on a triangular lattice interacting with an antiferromagnetic Heisenberg exchange J_H and coupled to an equal density of conduction electrons via a Kondo coupling J_K . This model is not sufficient to describe the physics of $x = 0.84$ cobaltate, because the ground state is predicted to be either a metal with an antiferromagnetically ordered moment (with nearest neighbor

spins forming a 120° angle) or a Kondo insulator, whereas the experiment requires a metallic ground state with ferromagnetic order in the plane. To see where the ferromagnetism comes from, we need to put in some numbers. The specific heat shows a peak at the magnetic transition T_N with a low temperature linear T coefficient γ of ≈ 10 mJ/Co-mole.[17] The extrapolation of the linear T contribution from above T_N gives $\gamma \approx 24$ mJ/Co-mole.[18] Assuming a spin unpolarized parabolic band, the latter value gives a mass $m^* = 35 m_e$. In a nearest neighbor tight binding fit to the band structure, this corresponds to a hopping matrix element $t_{eff} \approx 14$ meV. This is a factor of 6 or 7 mass enhancement compared with the typical tight binding fit to LDA bands. Coulomb repulsion is presumably responsible for this enhancement. Assuming this m^* and a hole density of $\frac{1}{13}$ carriers per Co, we obtain a Fermi temperature of 87 K. This exceptionally low energy scale has several important consequences.

First, in a narrow band with low energy, we expect a ferromagnetic tendency due to the Stoner mechanism, i.e., it is favorable to spin polarize to gain exchange energy at the expense of kinetic energy. Indeed, we believe that the ground state is fully spin polarized to form a “half-metal.” This will explain why the γ term in the specific heat drops by approximately a factor of 2 (from 24 to 10 mJ/Co-mole) across T_N . Furthermore, the *fully polarized* band has a Fermi surface area exactly equal to that of the reduced Brillouin zone (both equal to $\frac{1}{13}$ of the full zone). Intersection of an almost circular hole Fermi surface with a hexagonal reduced Brillouin zone (both equal to $\frac{1}{13}$ of the full zone) gives rise to small hole pockets and electron pockets, the latter being centered at the zone corner. Recently, L. Balicas and co-workers have observed small pockets in quantum oscillation studies of our $x=0.84$ crystals, which lends support to this picture.

The physical picture is that the ferromagnetic tendency among the conduction electrons opposes the Kondo coupling to form a singlet with the local moments, thereby suppressing the Kondo insulator state. The $S = \frac{1}{2}$ Heisenberg model on a triangular lattice is subject to strong quantum fluctuations and the 120° order may be greatly suppressed or eliminated entirely due to the Kondo coupling. The full many-body problem is a complicated one which deserves a separate study. In the supplementary information section we outline a simple mean field treatment which captures some features of the susceptibility.

Here we emphasize that the very small Fermi temperature helps explain the enhanced thermopower for $x = 0.84$. Conventional Sommerfeld theory predicts $S = (k_B/e)T/T_F$ for

$T < T_F$ and S is expected to roll over above T_F to a constant which depends on the classical configuration (the Heikes formula).[20] Experimentally, S shows a shallow peak around 100 K for $x = 0.84$ and the fit to low temperature Sommerfeld theory yields $T_F \approx 30$ K. We see that the crossover scale is about right and explains the success of the Heikes formula at these relatively low temperatures,[21] while the overall linear T slope and the magnitude need a factor of 3 enhancement compared with our estimate of $T_F \approx 87$ K. One possible source of enhancement is the deviation from a parabolic band because the band calculation shows severe flattening and even a dimple at the Γ point. Thermopower relies on the breaking of particle-hole symmetry, which is enhanced by a mass which decreases with increasing hole energy. Supporting evidence of this possibility comes from the observation that the low temperature γ term for the spin polarized band (10 mJ) is less than half of that extrapolated from high temperature (24 mJ). A second indication of the small Fermi energy comes from the Hall effect. The Hall constant R_H is predicted to be linear in $T > T_F$, a special consequence of hopping on a triangular lattice.[22] Experimentally R_H is linear in T above ~ 100 K, and saturates to a very small value at low temperature.[2] The latter may be a consequence of cancellations between the small electron and hole pocket mentioned earlier.

Optical measurements provide direct evidence for heavy mass and small carrier density. The low frequency conductivity consists of a broad peak centered around 150 cm^{-1} and a narrow Drude peak with a spectral weight estimated to be $\frac{1}{6}$ of that of the broad peak.[11, 12] We associate the broad peak with the hole bound to the Na vacancy. The Drude weight was estimated to correspond to $\omega_{\text{plasma}} = (4\pi n e^2 / m)^{\frac{1}{2}} \approx 1300 \text{ cm}^{-1}$ from which n/m can be extracted.[11] If we assume $m^* = 35m_e$, we find n to be even smaller (about $\frac{1}{3}$) than our estimate based on our model of 1/13 mobile carriers per Co. This extremely small Drude weight is very difficult to understand if all the holes are mobile.

Next we turn our attention to $x = 0.71$. This state, dubbed the ‘‘Curie-Weiss metal’’ is in many ways the most mysterious among all the doping concentrations. The T_N transition disappears and χ keeps rising with decreasing T . The resistivity $\rho(T)$ is linear down to ~ 4 K. The uniqueness of this behavior even in comparison with heavy fermion compounds has been emphasized by Li *et al.*[15]

The observation of Curie-Weiss behavior in a metal again calls for the coexistence of local moments and itinerant electrons. As an example, let us assume out of phase stacking of tri- and quadri- vacancies and that the quadri-vacancy binds a hole on each of the neighboring

Co planes, forming an $S = \frac{1}{2}$ local moment on each plane. The local moment forms a triangular lattice with one $S = \frac{1}{2}$ per 12 cobalt. For $x = 0.71$, the concentration of itinerant carriers is $2.5/12 \approx 0.208$ per Co, which is 2.7 times that of $x = 0.84$. We then expect a Fermi temperature of 235 K. The higher carrier density reduces the tendency towards Stoner instability, which explains the absence of a magnetic phase transition. In support of this picture, we note that in the thermopower, the saturation scale has moved to room temperature or above[3] and the fit of the low T data to $(k_B/e)T/T_F$ yields $T_F \approx 200$ K, consistent with our estimate and much larger than that for $x = 0.84$.

Finally, we note that a picture of conduction electrons coexisting with local moments which do not order down to the lowest temperature suggests the existence of a novel ground state for the spin system called the quantum spin liquid. While this possibility has been proposed in the literature,[23] there has been no known experimental realization. A system of $S = \frac{1}{2}$ on a triangular lattice coupled to a narrow band of conduction electrons with some ferromagnetic tendency may provide just the needed frustration to stabilize such a state. We note that spin liquid on a triangular lattice is expected to support a spinon Fermi surface,[24] with $\chi''(q, \omega)$ predicted to behave as[25]

$$\chi''(q, \omega) \approx \left[\left| |q| - Q_0 \right|^{3\sigma-1} + \left(\frac{\omega}{\omega_0} \right)^{\frac{2}{3}(3\sigma-1)} \right]^{-1} \quad (1)$$

where Q_0 is twice the spinon Fermi vector and σ is a critical exponent which was estimated to be 0.35 in a large N expansion. Equation (1) has unique signatures which can be tested by neutron scattering.

In conclusion, the observation of Na superlattice structure in the special Na concentrations of 0.84 and 0.71 show the importance of Na ordering in determining the unusual electronic properties. We have introduced a minimal model of local moments coexisting with itinerant electrons which accounts for many of the puzzling features observed in $x = 0.84$ and which forms the starting point for unraveling the mystery surrounding the ‘‘Curie-Weiss metallic’’ phase of $x = 0.71$. We believe exciting discoveries of exotic states of matter may lie ahead.

References

- [1] Takada, K. *et al.*, “Superconductivity in two dimensional CoO_2 layers,” *Nature* **422**, 53–55 (2003).
- [2] Foo, M.L. *et al.*, “Charge ordering, commensurability and metallicity in the phase diagram of the layered Na_xCoO_2 ,” *Phys. Rev. Lett.* **92**, 247001 (2004).
- [3] Lee, M. *et al.*, “Large enhancement of the thermopower in the Na_xCoO_2 at high Na doping,” *Nature Mater.* **5**, 537–540 (2006).
- [4] Bayrakci, S. *et al.*, “Magnetic ordering and spin waves in $\text{Na}_{0.82}\text{CoO}_2$,” *Phys. Rev. Lett.* **94**, 157205 (2005).
- [5] Mukhamedshin, I.R., Alloul, H., Collins, G. and Blanchard, N., “ ^{23}Na NMR Evidence for Charge Order and Anomalous Magnetism in Na_xCoO_2 ” *Phys. Rev. Lett.* **93**, 167601 (2004).
- [6] Ning, F.; Imai, T.; Statt, B. and Chou, F. “Spin dynamics in the carrier-doped $S = 1/2$ triangular lattice of $\text{Na}_x\text{CoO}_2 \cdot y\text{H}_2\text{O}$,” *Phys. Rev. Lett.*, **93**, 237201 (2004).
- [7] Zandbergen, H. W.; Foo, M. L.; Xu, Q.; Kumar, V. and Cava, R. J., “Sodium ion ordering in Na_xCoO_2 : Electron diffraction study”, *Phys. Rev. B* **70**, 024101 (2004).
- [8] Meng, Y. S.; der Ven, A. V.; Chan, M. K. Y. and Ceder, G. “Ab initio study of sodium ordering in $\text{Na}_{0.75}\text{CoO}_2$ and its relation to $\text{Co}^{3+}/\text{Co}^{4+}$ charge ordering,” *Phys. Rev. B*, **72**, 172103 (2005).
- [9] Roger M. *et al.*, “Patterning of sodium ions and the control of electrons in sodium cobaltate,” *Nature* **445**, 631–634 (2007).
- [10] T. Motohashi and E. Naujalis and R. Ueda and K. Isawa and M. Karppinen and H. Yamauchi, “Simultaneously enhanced thermoelectric power and reduced resistivity of $\text{Na}_x\text{Co}_2\text{O}_4$ by controlling Na nonstoichiometry”, *Appl. Phys. Lett.*, **79**, 1480 (2001).
- [11] Bernhard *et al.*, “Charge ordering and magnetopolarons in $\text{Na}_{0.82}\text{CoO}_2$,” *Phys. Rev. Lett.*, **93**, 167003 (2004).
- [12] Wang, N.L. *et al.*, “Infrared probe of the electronic structure and charge dynamics of $\text{Na}_{0.7}\text{CoO}_2$,” *Phys. Rev. Lett.* **93**, 237007 (2004) and Wu, D., Luo, J.L. and Wang, N.L., “Electron-boson mode coupling and the pseudogap of Na_xCoO_2 by infrared spectroscopy,”

- Phys. Rev. B **73**, 014523 (2006).
- [13] Chou, F. C.; Cho, J. H.; Lee, P. A.; Abel, E. T.; Matan, K. and Lee, Y. S., “Thermodynamic and Transport Measurements of Superconducting $Na_{0.3}CoO_2 \cdot 1.3H_2O$ Single Crystals Prepared by Electrochemical Deintercalation,” Phys. Rev. Lett. **92**, 157004 (2004).
- [14] Shu, G. J. *et al.*, “Searching for Sodium Ordered Phases in Single Crystal $\gamma - Na_xCoO_2$,” arXiv:0708.0280v1 [cond-mat.str-el], submitted to Phys. Rev. B.
- [15] Li, S.Y. *et al.*, “Giant electron-electron scattering in the Fermi-liquid state of $Na_{0.7}CoO_2$,” Phys. Rev. Lett. **93**, 056401 (2004).
- [16] Zhang, P. *et al.*, “Theory of sodium ordering in Na_xCoO_2 ,” Phys. Rev. B **71**, 153102 (2005).
- [17] Bayrakci, S.P. *et al.*, “Bulk antiferromagnetism in $Na_{0.82}CoO_2$ single crystals,” Phys. Rev. B **69**, 100410 (2004).
- [18] Luo, J.L. *et al.*, “Metamagnetic transition in $Na_{0.85}CoO_2$ single crystals,” Phys. Rev. Lett. **93**, 187203 (2004).
- [19] Qian, D. *et al.*, “Low-lying quasiparticle states and hidden collective charge instability in parent cobaltate superconductors,” Phys. Rev. Lett. **96**, 216405 (2006).
- [20] Chaikin, P.M. and Beni, G., “Thermopower in the correlated hopping regime,” Phys. Rev. B **13**, 647–651 (1976).
- [21] Mukerjee, S. and Moore, J., “Doping dependence of thermopower and thermoelectricity in strongly correlated systems,” arXiv:cond-mat/0609183.
- [22] Motrunich, O. and Lee, P.A., “Possible effects of charge frustration in $NaxCoO_2$: Bandwidth suppression, charge orders, and resurrected resonating valence bond superconductivity,” Phys. Rev. B **69**, 214516 (2004).
- [23] Senthil, T., Vojta, M. and Sachdev, “Weak magnetism and non-Fermi liquids near heavy-fermion critical points,” Phys.Rev. B **69**. 035111 (2004).
- [24] Lee, S.-S. and Lee, P.A., “U(1) gauge theory of the Hubbard model: Spin liquid states and possible application to κ -(BEDT-TTF) $_2$ Cu $_2$ (CN) $_3$,” Phys. Rev. Lett. **95**, 036403 (2005).
- [25] Altshuler, B.L., Ioffe, L.B. and Millis, A.J., “Low-energy properties of fermions with singular interactions,” Phys. Rev. B **50**, 14048 (1994).